Production of U-232 and U-233 in a fusion-fission hybrid

R. W. Moir

December 21, 2010

Abstract

One role for fusion is to produce fissile fuel for fission plants. Fissile fuel production can also be done with fission reactors but fusion can make an order of magnitude more fuel for the same total power making this use unique (8000 kg of ^{233}U /4400 $MW_{nuclear}$ from 3000 MW_{fusion} for a full power year). The fuel produced can be either ^{233}U or ^{239}Pu. Again, fusion is unique compared to fission in producing ^{233}U without Pu involved if desired. ^{233}U is useful in startup of thorium cycle fission plants and providing makeup fuel. While making ^{233}U, unusually large amounts of ^{232}U can be made, reducing the proliferation risk for thorium cycle use because ^{232}U has a daughter product that emits 2.6 MeV gamma rays. Fusion's 14 MeV neutrons by way of threshold reactions with a threshold of about 6 MeV make ^{232}U. Fission reactions have a small fraction of their neutrons born above 6 MeV but all fusion neutrons start out at 14.1 MeV from the D-T reaction, well above the 6 MeV threshold. This is another unique feature of fusion. While fission reactors on the thorium cycle might achieve $^{232}U/^{233}U$ ratios of about 0.1% at most, fusion can produce well in excess of 2.4% exceeding the IAEA standards of "reduced protection" or "self protection" set at a dose rate of 100 rem/h (1 Sv/h) 1 m from 5 kg of ^{233}U with 2.4% ^{232}U one year after chemical separation of daughter products. Three example breeding-blankets were studied. A hard spectrum blanket with no neutron multiplier gave $^{232}U/^{233}U$=7%. A design using liquid lithium as a neutron multiplier gave $^{232}U/^{233}U$=5% and when using beryllium as a neutron multiplier, $^{232}U/^{233}U$=4.5%. Another option is to produce ^{233}U that is 12% of uranium content ($^{233}U/U \leq 12\%$).

Table of Contents

Background and introduction

Fusion's role could be to use its neutrons to make fissile fuel for fission plants. Fusion's neutron being so energetic, 14.1 MeV, can and must be made to undergo reactions that multiply themselves because one neutron reaction is needed to replace the tritium consumed. Once multiplied, the slowed neutrons from fusion are not unique relative to fission neutrons. These neutrons can be absorbed in fertile material resulting in fissile material. The unique property of fusion's neutrons is to induce reactions that have threshold energy to take place.

In this report the reactions that produce ^{233}U and ^{232}U are discussed. Then we treat three distinct kinds of fission-suppressed blankets as examples to illustrate the unusually large ratios $^{232}\mathrm{U}/^{233}\mathrm{U}$ that can be achieved. These blankets are applicable to both magnetic fusion and inertial fusion. The emphasis is on ^{232}U production because of it role in nonproliferation in the context of the thorium fuel cycle in fission reactors.

^{232}U and ^{233}U production

Production of ^{233}U results from the reaction:

$$n + {}^{232}Th \rightarrow {}^{233}Th \rightarrow {}^{233}Pa + e^{-} \rightarrow {}^{233}U + e^{-}$$

Production of ^{232}U is the theme of this report. Four routes to producing ^{232}U are shown in Fig. 1 and are enabled by the three threshold reactions whose cross sections are shown in Fig. 2 and in the following two-step reactions:

1 $n + {}^{232}Th \rightarrow {}^{233}Th \rightarrow {}^{233}Pa + e^-$
$n + {}^{233}Pa \rightarrow 2n + {}^{232}Pa \rightarrow {}^{232}U + e^-$ (fast-neutron reaction)

2 $n + {}^{232}Th \rightarrow {}^{233}Th \rightarrow {}^{233}Pa + e^- \rightarrow {}^{233}U + e^-$
$n + {}^{233}U \rightarrow 2n + {}^{232}U$ (fast-neutron reaction)

3 $n + {}^{232}Th \rightarrow 2n + {}^{231}Th \rightarrow {}^{231}Pa + e^-$ (fast-neutron reaction)
$n + {}^{231}Pa \rightarrow {}^{232}Pa \rightarrow {}^{232}U + e^-$

Other reactions ending in ^{232}U are possible, such as the following three step-reactions:

4 $n + {}^{232}Th \rightarrow 3n + {}^{230}Th$ (fast-neutron reaction)
$n + {}^{230}Th \rightarrow {}^{231}Th \rightarrow {}^{231}Pa + e^-$
$n + {}^{231}Pa \rightarrow {}^{232}Pa \rightarrow {}^{232}U + e^-$

Still other less probable reactions ending in ^{232}U are possible:

5 $n + {}^{232}Th \rightarrow {}^{233}Th \rightarrow {}^{233}Pa + e^-$
$n + {}^{233}Pa \rightarrow {}^{234}Pa \rightarrow {}^{234}U + e^-$
$n + {}^{234}U \rightarrow 3n + {}^{232}U$ (fast-neutron reaction has low cross section)

The first four reactions listed above are shown in Fig. 1 as pathways with the same numbering.

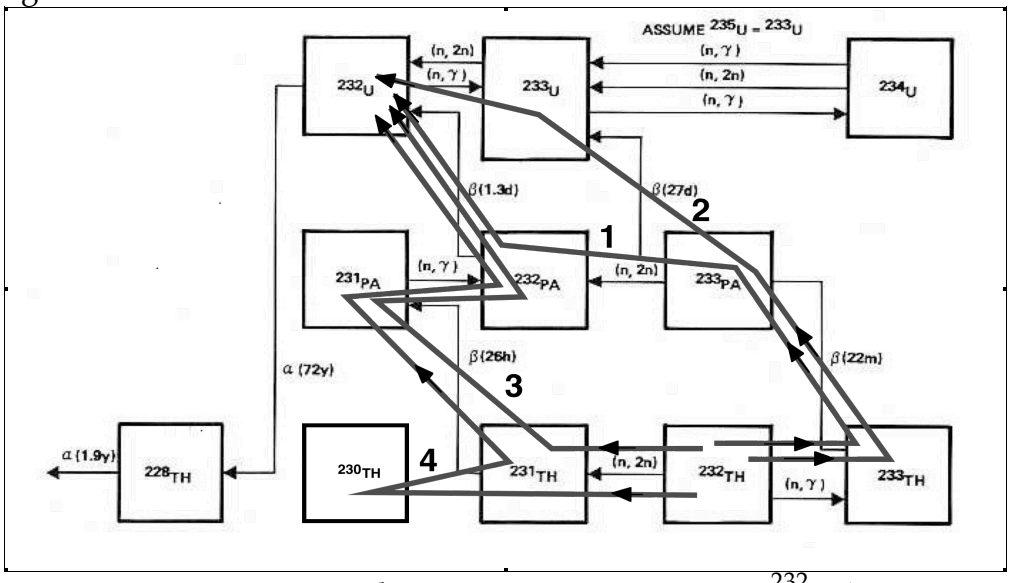

Fig. 1. Neutron reaction paths leading to production of ^{232}U (from Berwald et al. 1982, Fig VII.C-1).

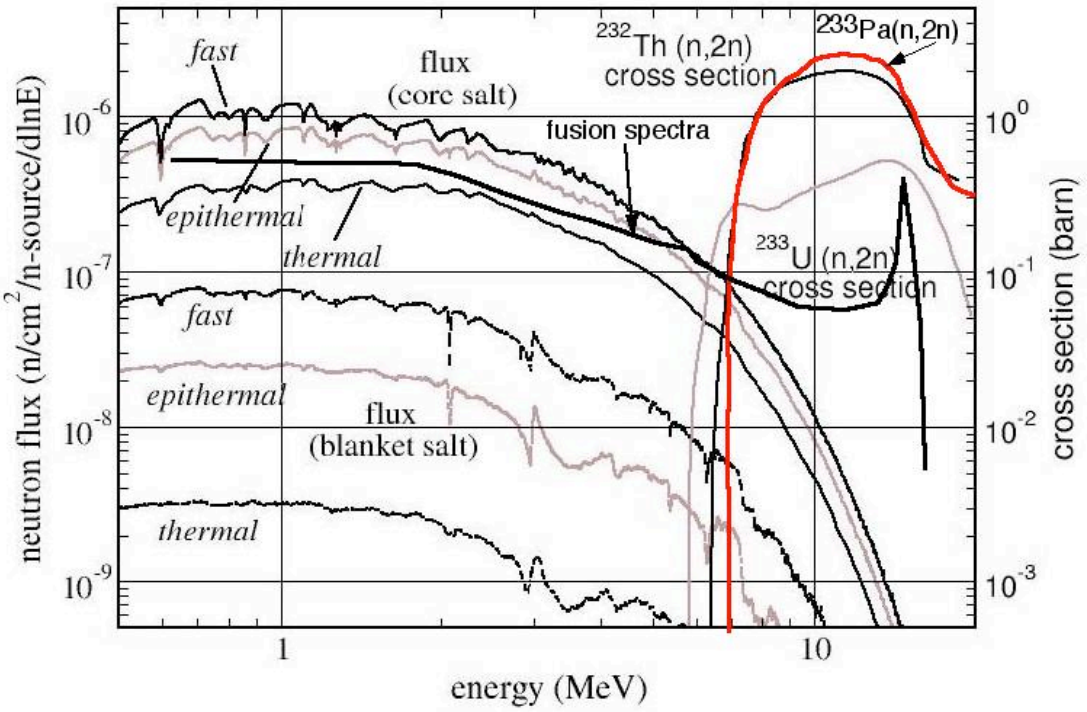

Fig. 2. Threshold cross-sections for producing ^{232}U, [Le Brun et al., 2005]. The fusion neutron spectrum is superimposed but not to scale vertically.

These reactions cannot take place with neutrons below 6 MeV. The fission process produces very few neutrons above 6 MeV but all of fusion's neutrons start out at 14.1 MeV. The production of ^{232}U therefore can be much greater for fusion sources than for fission sources of neutrons.

Since ^{231}Pa builds up, the first set of reactions depends on exposure time even after ^{233}U is removed. Long exposure times are useful and the Pa needs to be left in during processing to remove ^{233}U. The second reaction also depends on time during which the ^{233}U builds up to the value limited by processing rate to remove the produced material.

As the concentration of ^{232}U in ^{233}U builds up, detection becomes easier owing to the 2.6 MeV gamma activity as can be seen in the Fig. 3. As the concentration reaches several hundred ppm, being near a quantity of uranium such as 5 kg becomes dangerous. Above 2.4% (24,000 ppm) the activity becomes so high the IAEA's standard for reduced physical-protection or "self-protection" requirements (>100 rem/hr = 1 Sv/hr at 1 meter for 5 kg) are met [Kang and von Hipple, 2001, Table 2]. If we scale their result to 1 m we get 76.2 rem/h rather than 100 rem/h as quoted for 2.4% ^{232}U /^{233}U ($127\,rem/h \times \frac{2.4\%}{1\%} \times \left(\frac{0.5}{1.0}\right)^2 = 76.2\,rem/h$). This discrepancy is a topic to be resolved in the future.

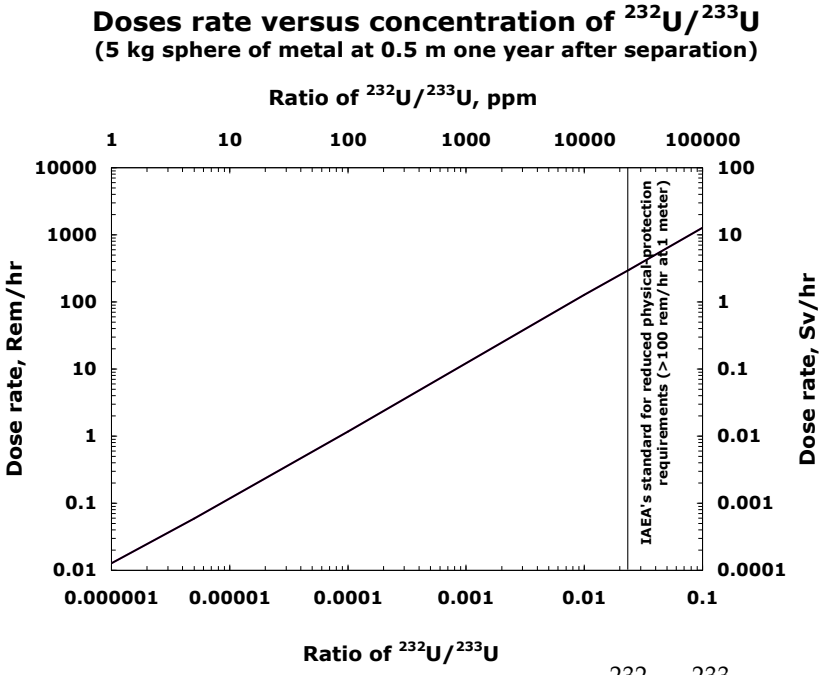

Fig. 3. Dose rate versus concentration of $^{232}U/^{233}U$.

We now proceed to estimate the concentrations of ^{232}U and ^{233}U that are produced in three example breeding blanket designs relevant to inertial and to magnetic fusion prospective power plants.

Rate of change of concentrations in molten salt

Molten salt is a convenient media to have the materials exposed to neutrons. Being a liquid the concentrations are continuously mixed and therefore spatially uniform. Also the liquid breeding media can accommodate complex geometry more readily than fuel rods and facilitate processing to remove bred uranium and tritium. The rate of change of concentrations and definitions are:

$$C_{Th} = \frac{^{232}Th\ atoms}{^{232}Th\ atoms} = 1$$

$$C_{Th2228} = \frac{^{228}Th\ atoms}{^{232}Th\ atoms}; \quad \frac{dC_{Th228}}{dt} = \lambda_{U2}C_{U232} - \lambda_{Th228}C_{Th228}$$

$$C_{Th230} = \frac{^{230}Th\ atoms}{^{232}Th\ atoms}; \quad \frac{dC_{Th230}}{dt} = R''_{Th}KC_{Th} - R'_{Th230}KC_{Th230}$$

At t=0, C_{Th230} = input value; ^{238}U decay results in ^{230}Th in nature[1].

$$C_{U2} = \frac{^{232}U\ atoms}{^{232}Th\ atoms}; \quad \frac{dC_{U2}}{dt} = R_{P1}KC_{P1} + R_{U3}KC_{U3} - R'_{U2}KC_{U2} + R_{P3}KC_{P3} - \lambda_{U2}C_{U2} - F^{U}\eta_{U}C_{U2} + R'_{U4}KC_{U4}$$

route #3,4 route #2 route #1

$$C_{U3} = \frac{^{233}U\ atoms}{^{232}Th\ atoms}; \quad \frac{dC_{U3}}{dt} = \lambda_{P3}C_{P3} - R'_{U3}KC_{U3} - F^{U}\eta_{U}C_{U3} + R_{U2}KC_{U2}$$

$$C_{U4} = \frac{^{234}U\ atoms}{^{232}Th\ atoms}; \quad \frac{dC_{U4}}{dt} = R''_{P3}KC_{P3} - R'''_{U4}KC_{U4} + R'''_{U3}KC_{U3} + R'_{U5}KC_{U5} - F^{U}\eta_{U}C_{U4}$$

$$C_{U5} = \frac{^{235}U\ atoms}{^{232}Th\ atoms}; \quad \frac{dC_{U5}}{dt} = R_{U4}KC_{U4} - R'''_{U5}KC_{U5} - F^{U}\eta_{U}C_{U5}$$

$$C_{P1} = \frac{^{231}Pa\ atoms}{^{232}Th\ atoms}; \quad \frac{dC_{P1}}{dt} = R'_{Th}KC_{Th} - R'_{P1}KC_{P1} + R''_{Th230}KC_{Th230} - \lambda_{P1}C_{P1} - F^{Pa}\eta_{Pa}C_{P1}$$

route #3 route #4

$$C_{P2} = \frac{^{232}Pa\ atoms}{^{232}Th\ atoms}; \quad \frac{dC_{P2}}{dt} = R_{P1}KC_{P1} + R_{P3}KC_{P3} - \lambda_{P2}C_{P2} - R_{P2}KC_{P2} - F^{Pa}\eta_{Pa}C_{P2}$$

C_{P2} quickly comes to equilibrium with its 1.31-day half-life. For $\frac{dC_{P2}}{dt} \approx 0$

$$C_{P2} \approx \frac{R_{P1}C_{P1} + R_{P3}C_{P3}}{R_{P2}K + \lambda_{P2} + F^{Pa}\eta_{Pa}}K$$

$$C_{P3} = \frac{^{233}Pa\ atoms}{^{232}Th\ atoms}; \quad \frac{dC_{P3}}{dt} = R_{Th}KC_{Th} - R'_{P3}KC_{P3} - \lambda_{P3}C_{P3} - F^{Pa}\eta_{Pa}C_{P3}$$

$\lambda_{P1} = decay\ rate\ of\ Pa231 = -(Ln0.5)/32{,}800\ y = 6.696 \times 10^{-13}\ s^{-1}$ clearly not important, Pa231 loss rate by decay is insignificant.

$\lambda_{P2} = decay\ rate\ of\ Pa232 = -(Ln0.5)/1.31\ d = 6.124 \times 10^{-6}\ s^{-1}$

$\lambda_{P3} = decay\ rate\ of\ Pa233 = -(Ln0.5)/27\ d = 2.97 \times 10^{-7}\ s^{-1}$

---

1. ^{230}Th also know as ionium exists in the presence of ^{238}U in equilibrium at 17 ppm owing to two alpha decays. Uranium is more soluble in water than thorium; that is the reason thorium that is often found with uranium can be "enriched" by one to three orders of magnitude in ^{230}Th (Somayajulu and Church, 1973). Also ^{230}Th could be recovered at considerable expense from uranium mine tailings. The initial value of C_{Th230} could be varied; however, ^{230Th} builds up to significant values.

$\lambda_{Pa234} = decay\ rate\ of\ Pa234 = -(Ln0.5)/6.69\ hr = 2.88 \times 10^{-5}\ s^{-1}$

$\lambda_{U2} = decay\ rate\ of\ U232 = -(Ln0.5)/70\ y = 3.14 \times 10^{-10}\ s^{-1}$
$\lambda_{Th228} = decay\ rate\ of\ Th228 = -(Ln0.5)/1.913\,y = 0.362\ y^{-1} = 1.148 \times 10^{-8}\ s^{-1}$
$\lambda_{Th230} = decay\ rate\ of\ Th230 = -(Ln0.5)/7.54 \times 10^{4}\ y = 9.19 \times 10^{-6}\ y^{-1}$
$\lambda_{Th231} = decay\ rate\ of\ Th231 = -(Ln0.5)/1.063\,d = 7.55 \times 10^{-6}\ s^{-1}$
$\lambda_{Th233} = decay\ rate\ of\ Th233 = -(Ln0.5)/22.3\text{min} = 5.18 \times 10^{-4}\ s^{-1}$

η_U=efficiency of removal of uranium isotopes, to be taken as 100% normally with fluorination.

η_{Pa}=efficiency of removal of protactinium isotopes, to be taken as 100% normally with reductive extraction.

F^U=fraction of molten salt processes per second=V per second processed/(V_{inside}+$V_{outside}$) for uranium removal, normally by fluorination.

F^{Pa}=fraction of molten salt processes per second=V per second processed/(V_{inside}+$V_{outside}$) for protactinium removal, normally by reductive extraction.

K=#neutrons/s ÷ number of Th atoms both inside and outside

The following reaction rates, denoted, R, are per 14.1 MeV neutron and for a nominal 1 molar fraction concentration of atoms per Th atom as computed by the TART neutron transport code using ENDFB-7 nuclear cross section data (Cullen, 2005). The calculations were done with a later version of the code. The concentrations of isotopes that build up are so low that the number of neutrons and their energy spectrum remain unchanged so that only one neutron transport calculation need be carried out. The differential equations then govern the concentrations changes with time.

R_{U2}=reactions per 14.1 MeV neutron, $^{232}U(n,\gamma)$

R'_{U2}=reactions per 14.1 MeV neutron that remove $^{232}U;(n,\gamma)$, (n,2n), (n,3n),….

R''_{U2}=reactions per 14.1 MeV neutron, $^{232}U(n, f)$

R_{U3}=reactions per 14.1 MeV neutron, $^{233}U(n,2n)$ route #2

R'_{U3}=reactions per 14.1 MeV neutron that remove ^{233}U; (n,γ), (n,2n), (n,f), …

R''_{U3}=reactions per 14.1 MeV neutron, $^{233}U(n, f)$

R'''_{U3}=reactions per 14.1 MeV neutron, $^{233}U(n, \gamma)$

R'''_{U4}=reactions per 14.1 MeV neutron that remove ^{234}U; (n,γ), (n,2n), (n,f), …

R_{U4}=reactions per 14.1 MeV neutron, $^{234}U(n, \gamma)$

R'_{U4}=reactions per 14.1 MeV neutron, $^{234}U(n,3n)$

R''_{U4}=reactions per 14.1 MeV neutron, $^{234}U(n,2n)$

R''''_{U4}=reactions per 14.1 MeV neutron, $^{234}U(n, f)$

R_{U5}=reactions per 14.1 MeV neutron, $^{235}U(n, \gamma)$

R'_{U5}=reactions per 14.1 MeV neutron, $^{235}U(n,2n)$

R''_{U5}=reactions per 14.1 MeV neutron, $^{235}U(n, f)$

R'''_{U5}=reactions per 14.1 MeV neutron that remove ^{235}U; (n,γ), (n,2n), (n,f), …

R_{P1}=reactions per 14.1 MeV neutron, $^{231}Pa(n,\gamma)$ route #3

R'_{P1}=reactions per 14.1 MeV neutron that remove ^{231}Pa; (n,γ), (n,2n), (n,3n)…

R''_{P1}=reactions per 14.1 MeV neutron, $^{231}Pa(n, f)$

R'_{P2}=reactions per 14.1 MeV neutron, $^{232}Pa(n, f)$

R_{P2}=reactions per 14.1 MeV neutron that remove ^{232}Pa; (n,γ),(n,2n), (n,3n),….

R_{Th}=reactions per 14.1 MeV neutron, $^{232}Th(n,\gamma)$

R'_{Th}=reactions per 14.1 MeV neutron, $^{232}Th(n,2n)$ route #3

R''_{Th}=reactions per 14.1 MeV neutron, $^{232}Th(n,3n)$ route #4

R'''_{Th}=reactions per 14.1 MeV neutron, $^{232}Th(n, f)$

R''''_{Th}=reactions per 14.1 MeV neutron that remove$^{232}Th(n,\gamma),(n,2n),(n,3n)$….

R_{Th230}=reactions per 14.1 MeV neutron, $^{230}Th(n, f)$

R'_{Th230}=reactions per 14.1 MeV neutron that remove ^{230}Th(n,γ),(n,2n),(n,3n)….

R''_{Th230}=reactions per 14.1 MeV neutron, ^{230}Th(n,γ)

R_{P3}=reactions per 14.1 MeV neutron, ^{233}Pa(n,2n) route #1

R'_{P3}=reactions per 14.1 MeV neutron that remove ^{233}Pa; (n,γ), (n,2n), (n,f), …

R''_{P3}=reactions per 14.1 MeV neutron, ^{233}Pa(n, γ)

R'''_{P3}=reactions per 14.1 MeV neutron, ^{233}Pa(n, f)

To see the size of each route shown in Fig. 1 do the following:

Route #1	run with $R_{P3}=0$	reduced ^{232}U is size of route #1
Route #2	run with $R_{U3}=0$	reduced ^{232}U is size of route #2
Route #3	run with $R'_{Th}=0$	reduced ^{232}U is size of route #3
Route #4	run with $R''_{Th}=0$	reduced ^{232}U is size of route #4

Energy from fission

The energy released per fusion neutron, E_0 is given by the TART code for the concentrations specified C^0. As the various concentrations change when solving he differential equations the changed energy from fission, E_f can be calculated:

$E = E_0 + E_f$

$$\begin{aligned} E_f = {} & 200\,MeV \times (R'''_{Th}(n,f) \bullet (C_{Th} - C^0{}_{Th}) + R_{Th230}(n,f) \bullet (C_{Th230} - C^0{}_{Th230}) \\ & + R''_{U2}(n,f) \bullet (C_{U2} - C^0{}_{U2}) + R''_{U3}(n,f) \bullet (C_{U3} - C^0{}_{U3}) + R''''_{U4}(n,f) \bullet (C_{U4} - C^0{}_{U4}) \\ & + R''_{U5}(n,f) \bullet (C_{U5} - C^0{}_{U5}) + R''_{P1}(n,f) \bullet (C_{P1} - C^0{}_{P1}) + R'_{P2}(n,f) \bullet (C_{P2} - C^0{}_{P2}) \\ & + R'''_{P3}(n,f) \bullet (C_{P3} - C^0{}_{P3}) \end{aligned}$$

The energy multiplication per 14.1 MeV neutron is:

$$M = \frac{E}{14.1\,MeV}$$

Molten salt characteristics

In our three example blankets to follow, each uses thorium dissolved in a different molten salt mixture given in Table 1.

Table 1
Parameters for molten salts

	75%LiF +25%ThF_4	72%LiF+16%BeF_2 +12%ThF_4	70%LiF+12%BeF_2 +18%ThF_4
Mole weight*	96.46	72.28	76.84
Mole wt thorium	58.01	27.85	41.77
ρ_{Molten} Salt. kg/m^3	3500	3350	3870
$\rho_{thorium}$, kg/m^3	2105	1290	2104
$K\frac{V}{P_f}$, 10^{-17}, $Ws^{-1}m^{-3}$	6.48	10.57	6.48
P_f, MW	500	3000	3000
V, m^3	95.3	1150	170
K, 10^{-10}, s^{-1}	3.44	2.76	11.4

*Natural Li is assumed.

The number of neutrons produced per unit time is:

$$\#n/s = \frac{500\ MW_f \times 0.8}{14.1\ MeV/n \times 1.602\times10^{-19}\ J/eV}\left(\frac{P_f}{500\ MW_f}\right) = 1.7707\times10^{20}\left(\frac{P_f}{500\ MW_f}\right) n/s$$

Each watt of fusion power produces 3.54×10^{11} n/s or 1.12×10^{19} n/y.

$$\frac{\#\ Th\ atoms}{kg\ of\ Th} = \frac{1\ Th\ atom}{232.038\ amu \times 1.6605\times10^{-27}\ kg/amu} = 2.595\times10^{24}\ Th\ atoms/kg\ of\ Th$$

$\#\ Th\ atoms = 2.595\times10^{24}\ Th\ atoms/kg \times \rho_{Th}V$, where V is the volume of molten salt both inside and outside the blanket and ρ_{Th} is the density of thorium in the molten salt.

$$K = \frac{\#n/s}{\#\ Th\ atoms\ total}$$

$$K = \frac{1.12\times10^{19}\ P_f\left(\frac{n}{Wy}\right)}{2.595\times10^{24}\ Th\ atoms/kgTh\ \rho_{Th}V} = 4.32\times10^{-6}\frac{P_f}{\rho_{Th}V}\,y^{-1} \quad or$$

$$= \frac{3.54\times10^{11}\ P_f\left(\frac{n}{Ws}\right)}{2.595\times10^{24}\ Th\ atoms/kgTh\ \rho_{Th}V} = 1.365\times10^{-13}\frac{P_f}{\rho_{Th}V}\,s^{-1}$$

Some calculations useful for the various examples are given in the footnote[2].

Specific fission-suppressed ^{233}U breeding blankets using molten salt

In the next sections we treat three example blankets for producing ^{233}U. They are fission-suppressed in the sense that we remove the breed ^{233}U before it has a chance to significantly fission. Fast-fission is minimized by making the fertile material dilute. Each uses molten salt that keeps spatially uniform concentrations of materials because it is a liquid and can conform to complex geometry, a feature that is difficult with solid fuel rods, and finally because the liquid fuel eases processing. By designing to suppress fission more fusion neutrons are available to breed for a fixed total thermal power and fission power is generally found in paper studies to be produced more economically in fission reactors than in fusion reactors unless the electrical power is large, >3 GWe.

All molten salt blanket, MS

The molten salt blanket consists of a spherical shell of molten salt shown in Fig. 4.

$$V_{inside} = \frac{4}{3}\pi(3^3 - 2.5^3) = 47.65\ m^3$$

---

2. The molecular weight is:

$$M = LiF_{\frac{3}{4}} + ThF_{4\ \frac{1}{4}} = (6.941 + 18.998)_{\frac{3}{4}} + (232.04 + 4 \times 18.998)_{\frac{1}{4}} = 96.462\ g/mole$$

$$\frac{6.025 \times 10^{23}\ molecules/mole}{96.462\ g/mole} = 6.246 \times 10^{21}\ molecules/g\ of\ molten\ salt$$

$$6.246 \times 10^{21}\ molecules/g \times 3500\ kg/m^3 \times 0.25\ Th\ atoms/molecule = 5.465 \times 10^{27}\ Th\ atoms/m^3$$

$$6.246 \times 10^{21}\ molecules/g \times 0.25\ Th\ atoms/molecule = 1.5615 \times 10^{24}\ Th\ atoms/kg\ MS$$

$$5.465 \times 10^{27}\ Th\ atoms/m^3 \times 47.65\ m^3 = 2.604 \times 10^{29} \cdots Th\ atoms\ inside\ blanket$$

$$5.465 \times 10^{27}\ Th\ atoms/m^3 \times 232 amu/Th\ atom \times 1.66 \times 10^{-27} kg/amu = 2106\ kg\ Th/m^3$$

$$Total\ Th\ atoms = \frac{V_{inside} + V_{outside}}{V_{inside}} 2.604 \times 10^{29} \cdots Th\ atoms\ inside\ and\ outside\ the\ blanket$$

$$K = \frac{1.7707 \times 10^{20}\left(\frac{P_f}{500MW_f}\right) n/s}{\frac{V_{inside} + V_{outside}}{47.65} 2.604 \times 10^{29}}$$

$$= \frac{3.283 \times 10^{-8}\left(\frac{P_f}{500MW_f}\right) \times \frac{Th\ atoms/molecule}{0.25} s^{-1}}{V_{inside} + V_{outside}}$$

$= 3.44 \times 10^{-10}\ s^{-1}$ for the inertial example.

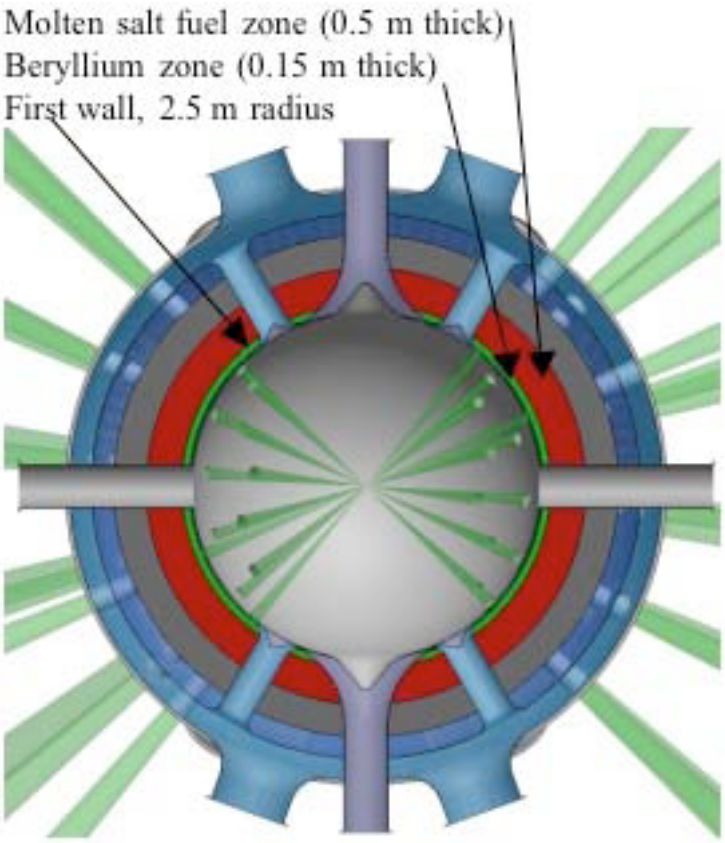

Fig. 4. Inertial fusion blanket, LIFE (Moses et al, 2009).

$V_{outside}$ = volume of molten salt in piping and processing equipment outside of the neutron flux and is taken as equal to the volume inside, so V=95.3 m^3 and assumes 2.5 m^3/d processing rate for uranium removal. The entire inventory is processed in 38 days. The molten salt was a 0.5 m spherical shell starting at 2.5 m followed by a 0.5 m layer of graphite. The molten salt was 75% LiF and 25% ThF_4 plus small amounts of other resulting isotopes that evolve with time. ^{6}Li is 53.3% of lithium and TBR=1.025 and F=0.236, where TRB is the tritium breeding ratio and F is the fissile breeding ratio per 14.1 MeV neutron. ρ=3500 kg/m^3 ρ_{Th}=2100 kg/m^3. The 95.3 m^3 of molten salt contains 200 tonnes of thorium. The material percentages in the molten salt for the neutron transport calculations are:

Table 2
Material percentages for MS case

Element	Atom, %
6Li	40
7Li	35
19F	175
230Th	0.025
232Th	25
231Pa	0.025
232Pa	0.0025
233Pa	0.025
232U	0.0025
233U	0.025
234U	0.025
235U	0.0025

The sense of the numbers in Table 2 are for example: C_{Th230}= 0.025%/25% =0.001. The fusion power is 500 MW and the first wall is at 2.49 m giving a neutron wall load of 5.1 MW/m^2.

Neutron transport cases were run for the spherical shell just described with the graphite reflector and for a much thicker molten salt zone, that is, an infinite media case. There was no first wall or structural material in the calculation. Both are shown in Table 3 and the infinite media case in Fig. 5.

These results are inaccurate owing to the lack of holes in the blanket, to the absence of structure, and no first wall. Also, the tritium-breeding ratio is too low and needs to be increased possibly by increasing the $^6Li/^7Li$ ratio or adding a neutron multiplier as in our other two example blankets. Nevertheless, the calculations result in an astoundingly large production of ^{232}U, 2.4% after 2.5 years and over 7% of ^{233}U after about ten years of exposure and continues to climb owing to the buildup of ^{231}Pa.

Table 3
Parameters and neutron transport results for three example blankets

	MS, C reflector	MS-infinite	Li/MS Sphere	Li/MS-cyl	Be/MS-Sphere	Be/MS-cyl
P_{fusion}, MW	500	500	3000	3000	3000	3000
V_{inside}, m^3	47.65	47.65	1052	1052	85	85
$V_{outside}$, m^3	47.65	47.65	100	100	85	85
Process rate, m^3/d	2.5	2.5	14.4	14.4	10	10
F^U, 10^{-7} s^{-1}		3.036		1.447		6.808
^6T	0.968	0.993	0.48	0.528	1.073	1.123
$^7T/T$	0.058/1.025	0.060/1.053	0.63/1.12	0.679/1.21	0.023/1.10	0.0242/1.147
F(Th[n,g])	0.236	0.254	0.564	0.515	0.730	0.780
T+F	1.260	1.306	1.680	1.72	1.826	1.927
K, 10^{-10}	3.4	3.4	2.76	2.76	11.4	11.4
M (E/14.1)	1.76	1.79	1.49	1.44	2.108	2.166
R_{P1} n,γ	1.0	1.05	14.1	12.85	21.9	23.56
R'_{P1} all	1.45	1.52	14.2	12.91	22.0	23.64
R''_{P1} n,f	0.30	0.32	0.06	0.051	0.044	0.052
R'_{P2} n,f	1.40	1.41	19.7	17.53	54.7	57.5
R_{P2} all	2.03	1.03	26.7	81.91	81.91	85.85
R_{P3} n,2n	0.221	0.21	0.030	0.025	0.033	0.028
R'_{P3} all	1.41	1.48	10.49	9.63	9.82	10.6
R''_{P3} n,γ	1.090	1.14	10.4	9.59	9.78	10.6
R'''_{P3} n,f	0.09	0.097	0.017	0.014	0.013	0.015
R_{U2} n,γ	0.38	0.43	3.25	2.98	4.1	4.65
R'_{U2} all	2.12	1.95	10.55	9.84	10.9	11.78
R''_{U2} n, f	1.45	1.51	7.3	6.86	6.8	7.13
R_{U3} n,2n	0.025	0.007	0.005	0.0034	0.005	0.0036
R'_{U3} all	2.26	2.38	16.09	14.55	31.0	32.65
R''_{U3} n,f	2.02	2.12	13.9	12.56	27.7	29.2
R'''_{U3} n,γ	0.22	0.23	2.2	1.98	3.2	3.44
R''_{U4} n,2n	0.04	0.050	0.01	0.0069	0.006	0.0067

	MS, C reflector	MS-infinite	Li/MS Sphere	Li/MS-cyl	Be/MS-Sphere	Be/MS-cyl
R'_{U4} n,3n	0.00035	0.0004	<0.005	0.00001	<0.0005	0.00004
R_{U4} n,γ	0.32	0.32	7.8	7.19	9.81	10.5
R''''_{U4} n,f	0.48	0.50	0.11	0.09	0.075	0.085
R'''_{U4} all	0.85	0.87	7.95	7.28	9.89	10.608
R_{U5} n,γ	0.38	0.40	3.36	2.99	3.25	5.37
R'_{U5} n,2n	0.069	0.062	0.013	0.007	<0.05	0.0093
R''_{U5} n,f	1.48	1.54	8.73	7.84	23.5	24.8
R'''_{U5} all	1.93	2.00	12.1	10.83	28.3	30.19
R_{Th} n,γ	0.236	0.254	0.564	0.515	0.730	0.780
R'_{Th} n,2n	0.188	0.196	0.034	0.0246	0.0256	0.0267
R''_{Th} n,3n	0.051	0.052	0.0037	0.00229	0.0052	0.0054
R'''_{Th} n,f	0.051	0.053	0.0087	0.00636	0.0073	0.0076
R''''_{Th} all	0.525	0.55	0.611	0.548	0.768	0.8198
R_{Th230} n, f	0.094	0.10	0.016	0.013	0.014	0.014
R''_{Th230} n,γ	0.132	0.11	8.75	8.03	8.99	9.97
R'_{Th230} all	0.433	0.43	8.79	8.07	9.04	10.0
R_{U238} n,γ						0.023
R_{U238} n, f						3.15
R_{Pu239} n,γ						49.5
R_{Pu239} n, f						29.5
R_{Pu240} n,γ						92.2
R_{Pu240} n, f						0.12
Neutron histories	$2x10^7$	$2x10^7$	10^7	107	$2x10^6$	$2x10^8$

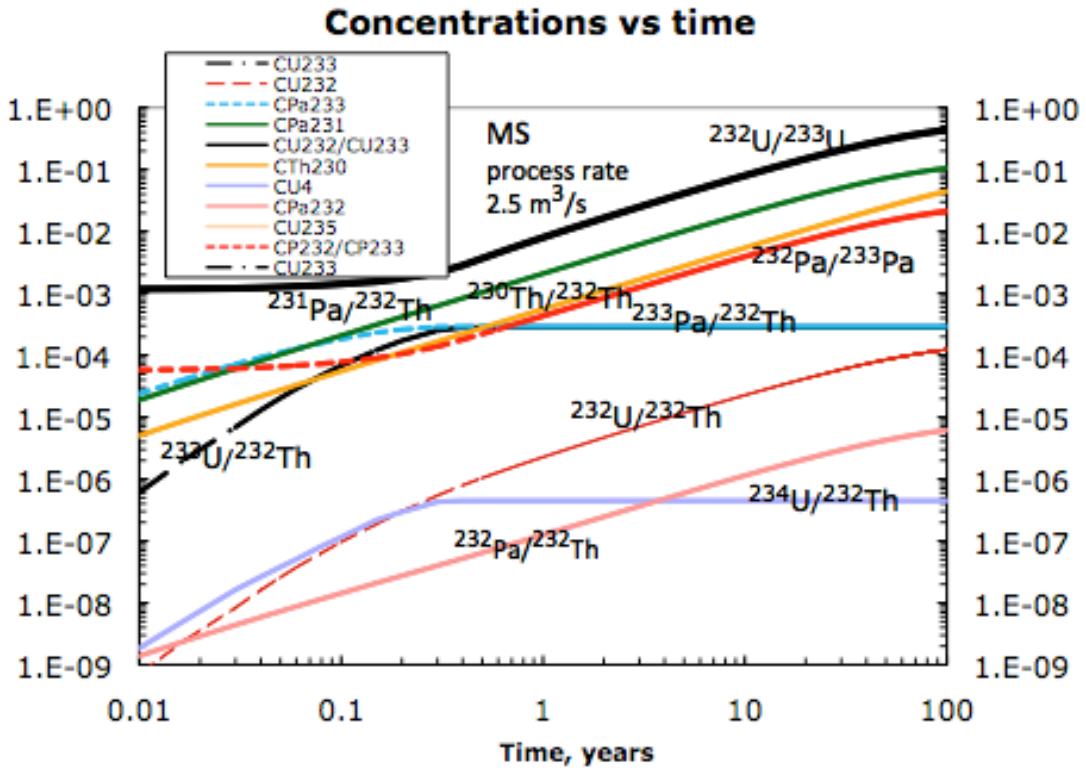

Fig. 5. Concentration ratios, especially $^{232}U/^{233}U$ versus exposure time for the infinite media MS blanket case.

The contribution to the $^{232}U/^{233}U$ ratio from each route is given in Table 4.

Table 4
Contribution to the $^{232}U/^{233}U$ ratio in % MS

Time, y	Route #1 $^{233}Pa(n,2n)$	Route #2 $^{233}U(n,2n)$	Route #3 $^{232}Th(n,2n)$	Route #4 $^{232}Th(n,3n)$
0.05	18.6	0.054	81.0	0.0005
0.1	16.8	0.12	82.8	0.00097
0.2	14.3	0.2	85.5	0.0019
0.5	8.7	0.37	90.9	0.0055
1	4.4	0.44	95.1	0.012
5	0.69	0.18	99.1	0.07
10	0.32	0.09	99.4	0.16
20	0.16	0.045	99.4	0.33

Redo above numbers with final results—only small changes expected

Clearly, route #3 is the most important at all times and route #1 has some importance but only at early times less than one year. Another important observation is that even for early times less than one year the $^{232}U/^{233}U$ ratio is over 0.1% and exceeds 2.4% after 2.5 years of exposure.

The importance of the processing rate is to limit the buildup of ^{233}U to limit the fission rate. The idea is that the hybrid is the "best" place to breed and fission reactors are the "best" place to produce power. A plot of energy released per fusion neutron versus the $^{233}U/^{232}Th$ ratio will show when fissioning becomes important.

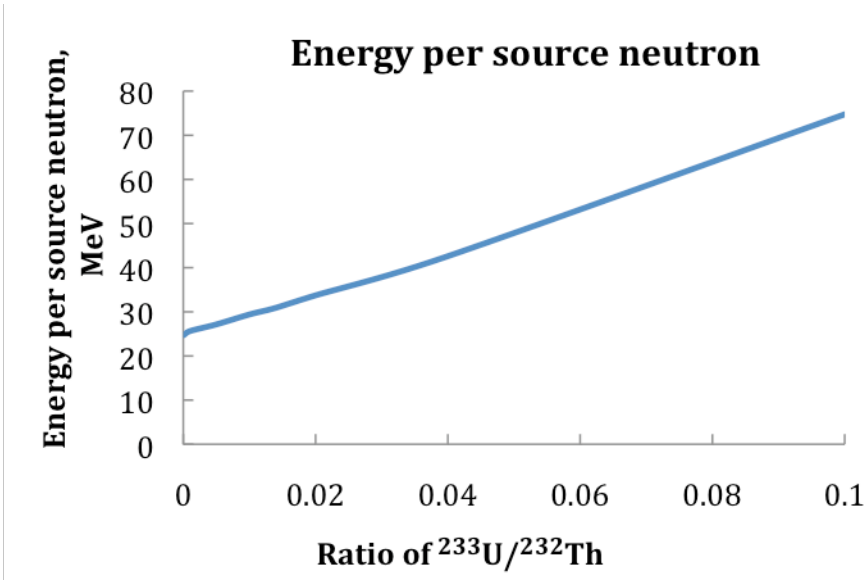

Fig. 6. Energy per source neutron versus ratio of $^{233}U/^{232}Th$.
Probably delete or replace this figure.

If the energy release with no ^{233}U is 24.74 MeV, then it increases by 3.6% for $^{233}U/^{232}Th$= 0.001 and by 10% for $^{233}U/^{232}Th$= 0.005 and for $^{233}U/^{232}Th$=0.01 the increase is 19%. Decide if to use or not.

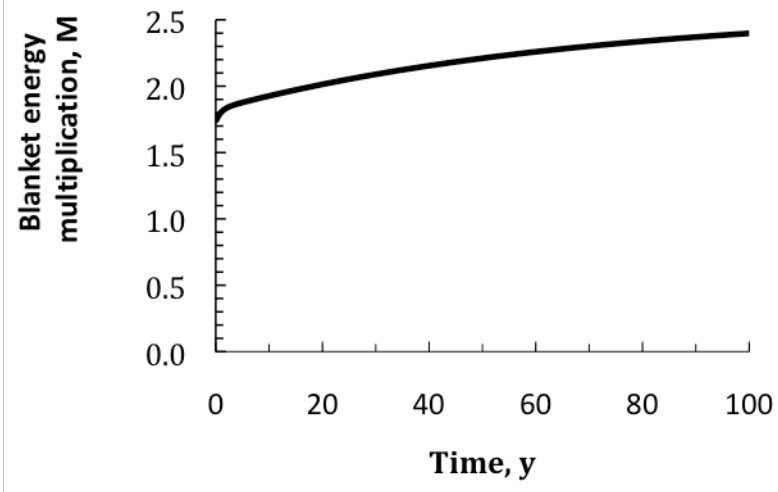

Fig. 7. Blanket energy multiplication increases owing to fission of built up materials.

At 100 y the contributions are 6 MeV for Pa-132, 1.6 MeV for U-233, 1 MeV for Th-230 that accounts for most of the rise above. The processing rate to remove uranium isotopes was 2.5 m^3/d that processes the entire blanket inventory in 381 days.

The above results based on spherical shell of molten salt 0.5 m thick are based on the infinite media results and therefore are applicable to a long cylinder appropriate to a magnetic mirror fusion neutron source or a tokamak case. A tandem mirror configuration could have a liquid (molten salt, not liquid metal because of MHD effects for a conducting media) first wall (Moir and Rognlien, 2007). End neutron leakage is small because the length is so great.

The case has such low breeding (F=0.25 ^{233}U atoms per 14.1 MeV neutron) that it is not very practical and needs a neutron multiplier. See the next two examples with ^{7}Li and Be as neutron multipliers. Steady state is not achieved for most of the materials.

Li neutron multiplier, molten salt breeder, Li/MS

A well-documented tandem mirror fusion breeder design is modeled (Lee, Berwald et al, 1982, herein after referred to as Berwald, Chapter VII, 1982). Considerable attention was given to ^{232}U production. A spherical shell model was used for a first approximation but most of the results were for cylindrical geometry. The first wall of 10 mm thickness is located at 2.5 m radius followed by 0.5 m of liquid lithium as a tritium breeder and neutron multiplier out to 3.0 m, followed by 0.5 m of molten salt to 3.5 m, followed by 0.5 m graphite reflector. Our calculation assumes V_{inside}=1050 m^3, $V_{outside}$ =100 m^3. One calculation with a processing rate of 14.4 m^3/d was made (80 days to process the entire inventory for uranium). The molten salt was LiF 72%+BeF_2 16%+ThF_4 12% plus small amounts of other resulting isotopes that evolve with time. ^{7}Li is 99.08% of the lithium in the liquid lithium zone, almost all ^{7}Li in the molten salt zone, and TBR=1.13 and F=0.605. The calculations of reactions per source neutron were done with the TART code with no Fe using both a spherical shell model and a cylindrical model. The 10 mm Fe first wall was at 2.49 m, a lithium zone extended from 2.5 m to 3.0 m and contains 0.92% Li-6 and 99.08% Li-7. There should have been an Fe wall of 10 mm or more to 3.01 m, a molten salt zone extended to 3.5 m, and there should have been another 10 mm Fe wall followed by 0.5 m of C. The amount of thorium is 1,484 tonnes. However, no Fe was used.

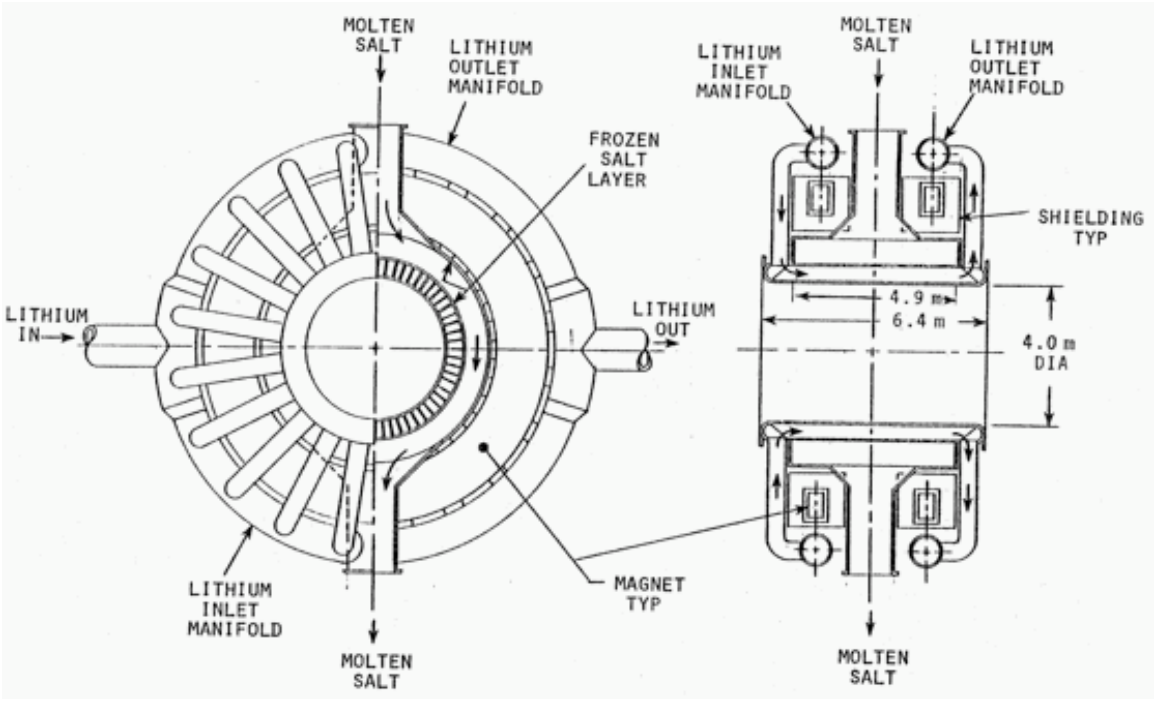

Figure 8. Two zone lithium neutron multiplier blanket with a molten salt second zone for the breeding media (Berwald et al, 1982).

Table 5
Material percentages for Li/MS case

Element	Atom %, t=0	Atom %, t=∞	Fission energy, MeV
6Li	0.00001	0.00001	
7Li	72	72	
9Be	16	16	
19F	152	152	
228Th	0	1.641×10^{-5}	
230Th	0.012	0.00341	0.0007
232Th	12	12	1.3
231Pa	0.012	0.025	0.02
232Pa	0.0012	0.0000145	0.004
233Pa	0.012	0.00571	0.0013
232U	0.0012	0.00060	0.07
233U	0.012	0.0114	2.4
234U	0.012	0.000145	0.0002
235U	0.0012	1.97×10^{-6}	0.00025

The results are shown in Table 3 and Fig. 9 with the initial and final conditions for U processing only are given in Table 5.

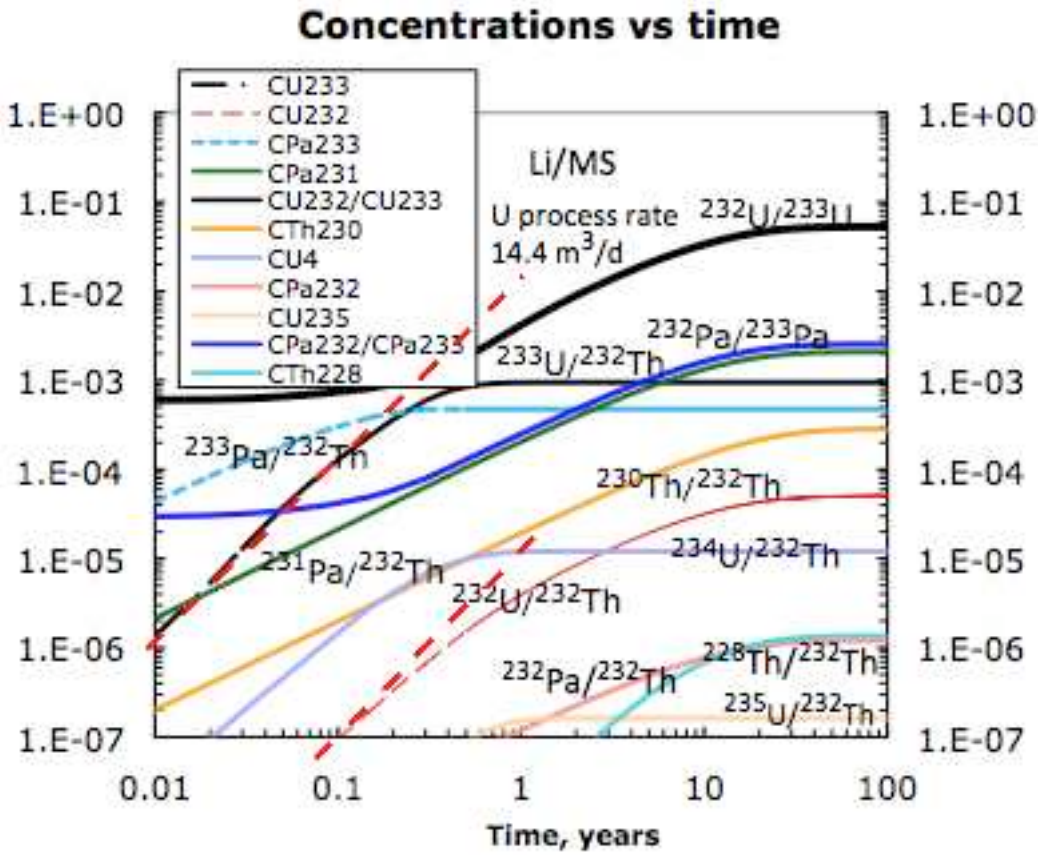

Fig. 9a. Concentration ratios versus exposure time for the Li/MS cylindrical mirror fusion case, uranium processing only.

In order to compare with Berwald, 1982 we ran a case with Pa processing as well; however, for nonproliferation reasons we do not recommend this case.

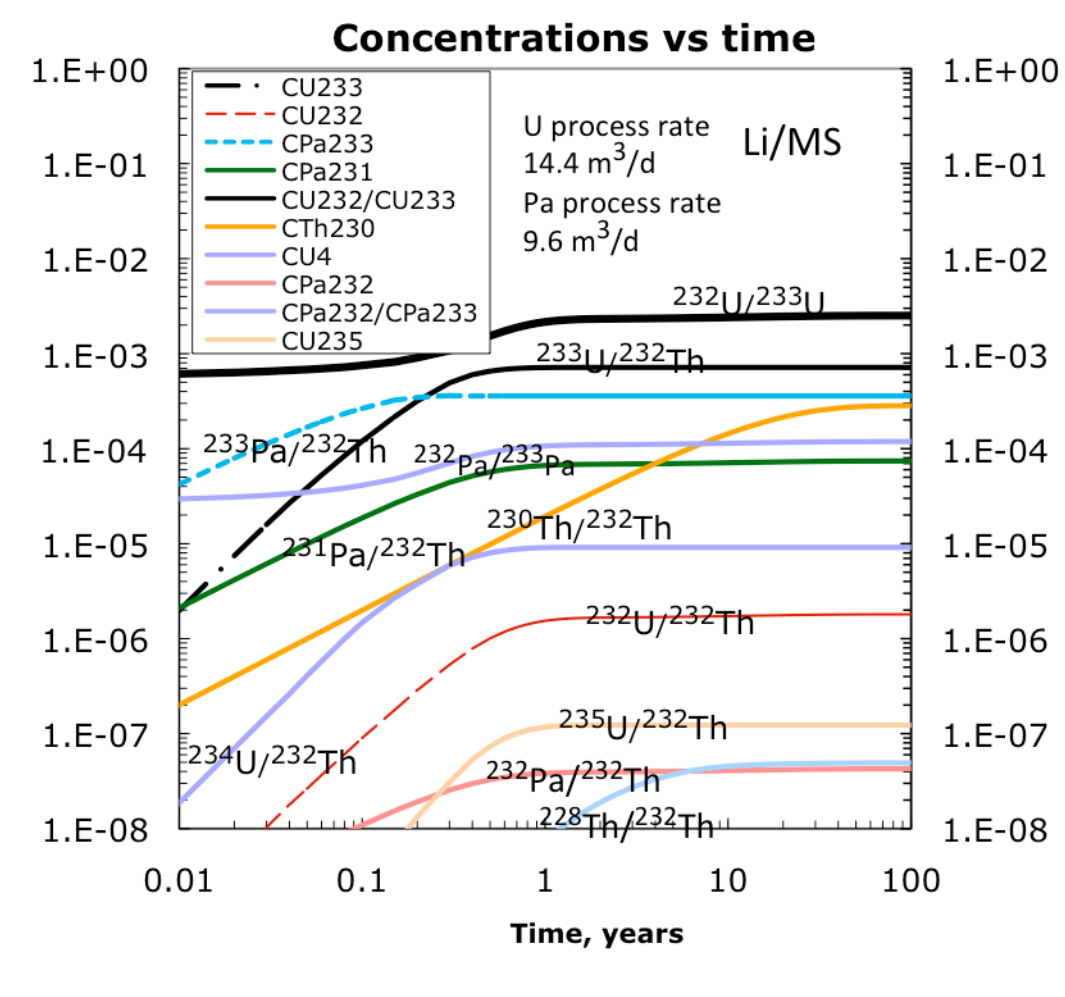

Fig. 9b. Concentration ratios versus exposure time for the Li/MS cylindrical mirror fusion case, both uranium and protactinium processing.

In order to compare with Berwald, 1982 we also ran a case with no processing.

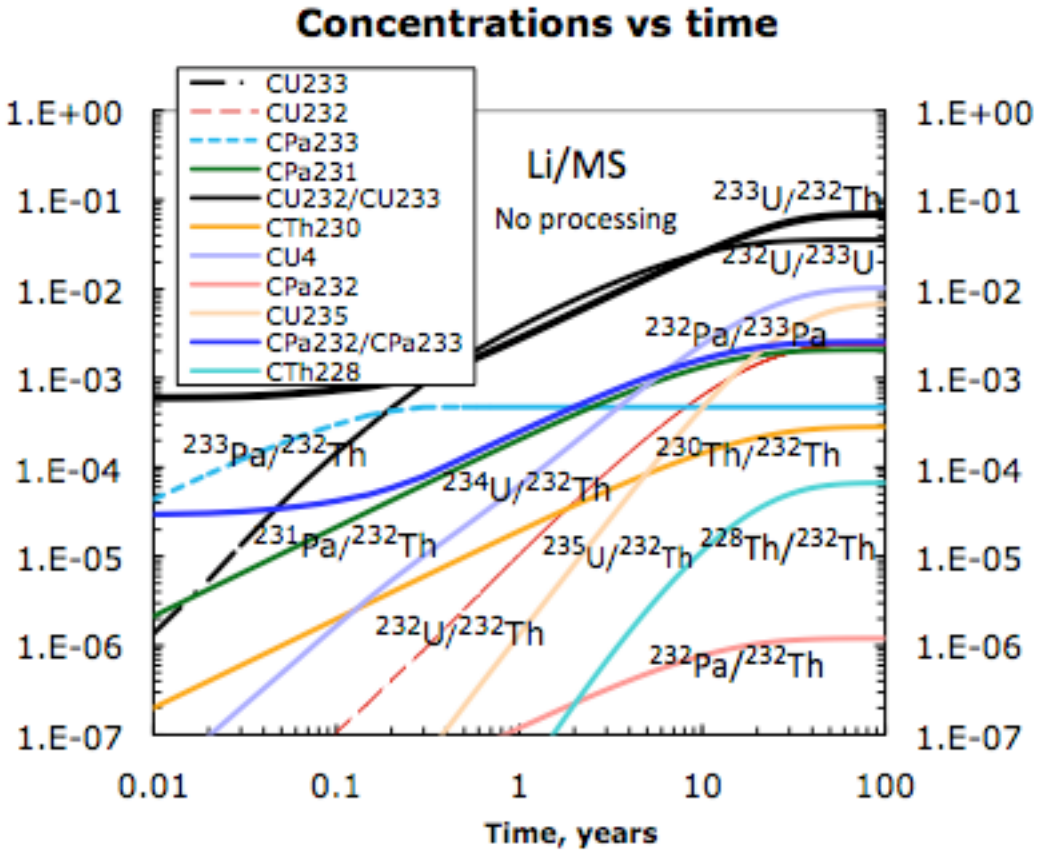

Fig. 9c. Concentration ratios versus exposure time for the Li/MS cylindrical mirror fusion case, with no processing.

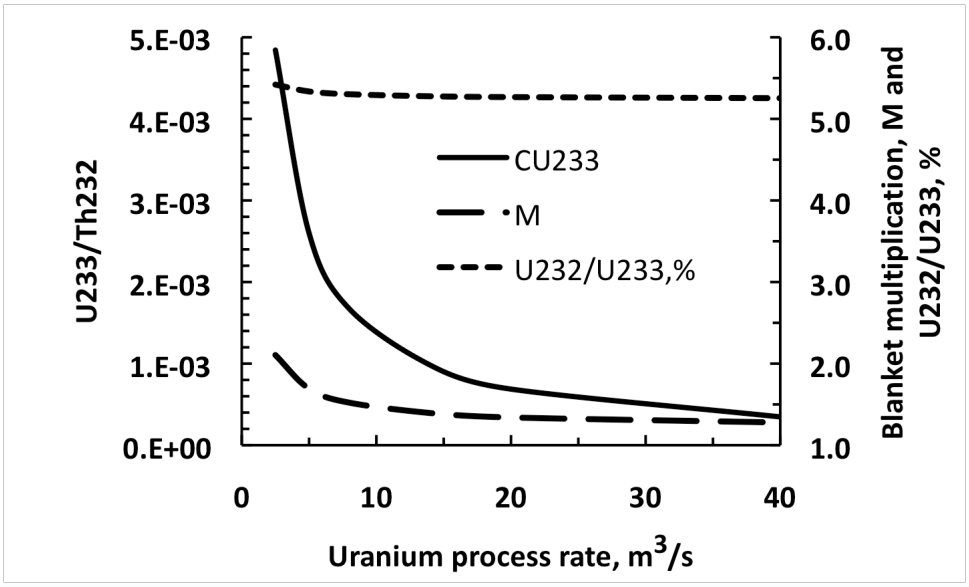

Fig. 10. Effect of varying process rate.

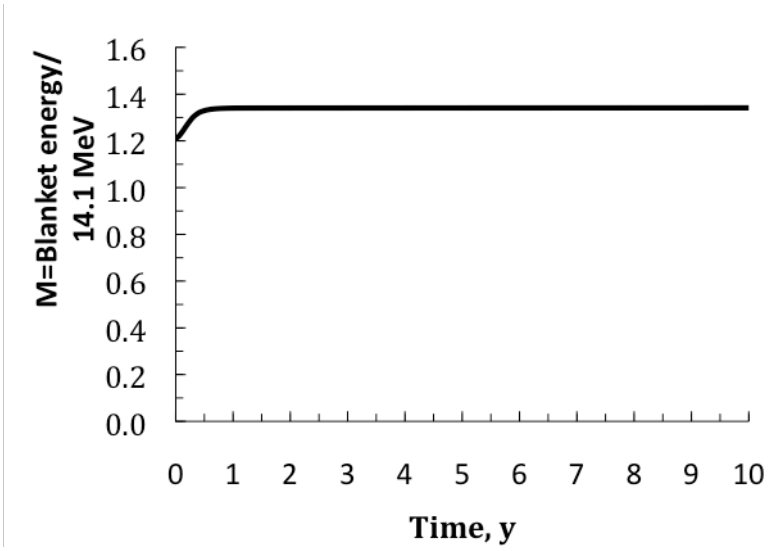

Fig. 11. Blanket energy multiplication vs time.

Table 6
Contribution to the $^{232}U/^{233}U$ ratio in %
Li/MS **Redo these numbers with final results—only small changes are expected**

Time, y	Route #1 $^{233}Pa(n,2n)$	Route #2 $^{233}U(n,2n)$	Route #3 $^{232}Th(n,2n)$	Route #4 $^{232}Th(n,3n)$
0.05	4.0	0.02	95.6	0.01
0.1	3.5	0.03	96.3	0.02
0.2	2.9	0.05	97.0	0.03
0.5	1.5	0.08	98.4	0.09
1	0.6	0.05	99.1	0.2
5	0.1	0.01	98.7	1
10	0.08	0.006	97.7	2.2
20	0.06	0.004	95.8	4

The Li/MS case is for a Tandem Mirror with Berwald's results shown in Fig. 12a, b and c.

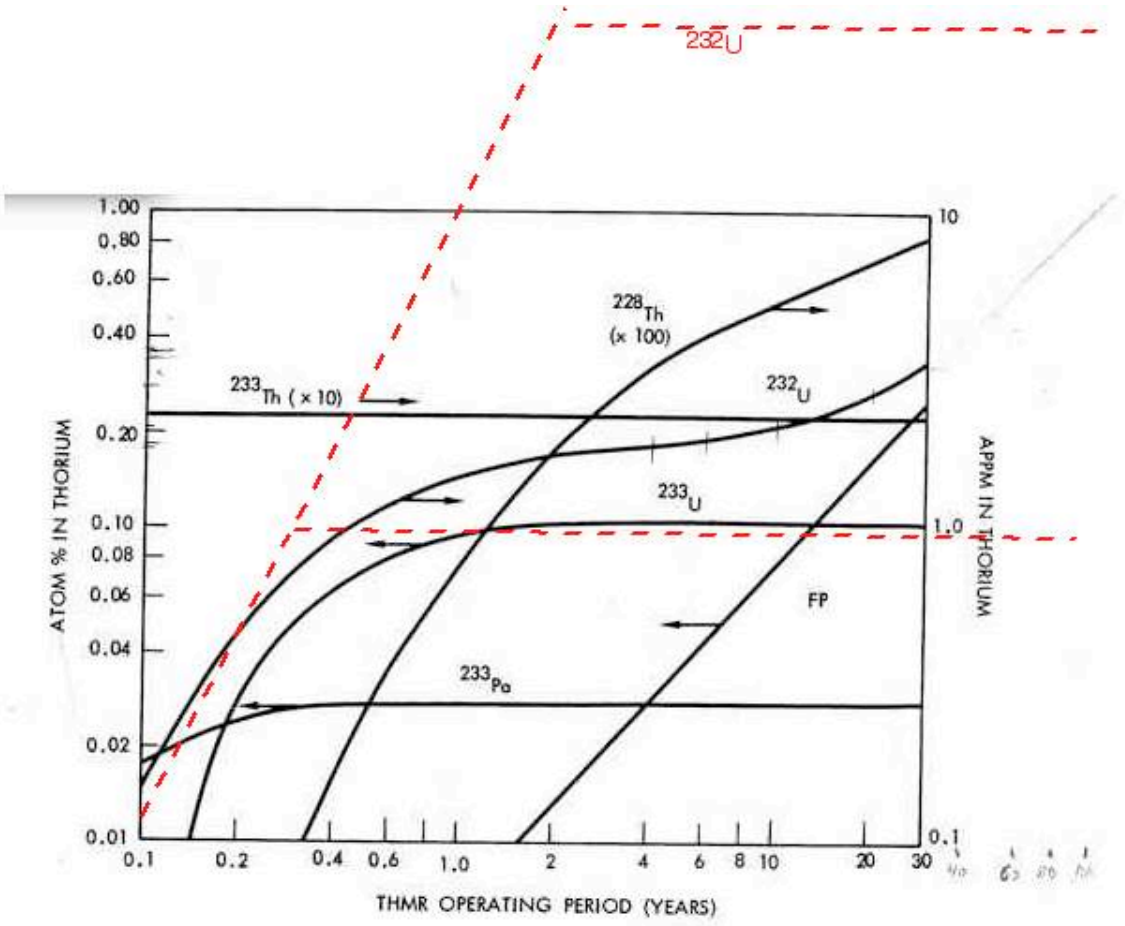

FIGURE VII.C-4. Isotopic generation in the molten salt blanket TMHR for fluorination only reprocessing mode.

Fig. 12a. Berwald's calculations for the Li/MS case with uranium processing at 0.6 m^3/h=14.4 m^3/d from Berwald 1982, p.VII-78. Berwald's plant operated 70% of the time. The red dashed lines are from the appendix based on 100% capacity factor. Berwald's U-233 production is about a factor of 50 below the present calculations. No explanation for the discrepancy has been found.

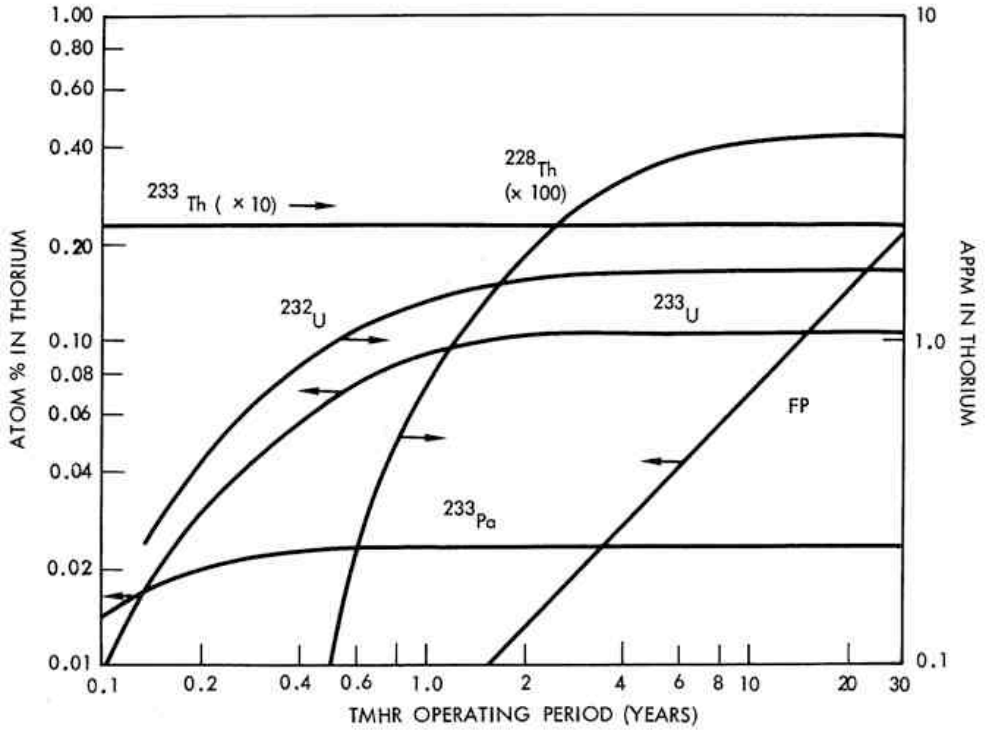

FIGURE VII.C-5. Isotopic generation in the molten salt blanket for full reprocessing mode.

Fig. 12b. Berwald's calculations for the Li/MS case with both uranium and protactinium processing (0.35 m^3/h=8.4 m^3/d at 100% capacity factor).

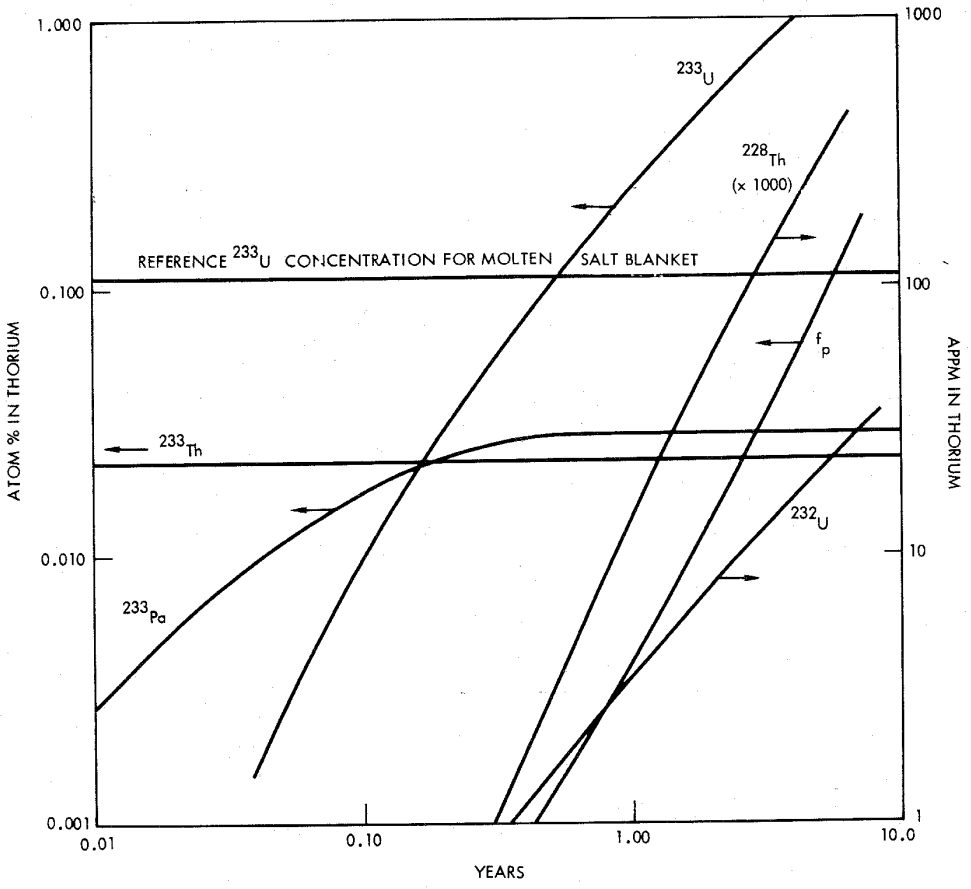

FIGURE VII.A-3. Isotopic generation in molten salt blanket with no fuel reprocessing (batch mode).

Fig. 12c. Berwald's calculations for the Li/MS case with no processing.

In Berwald's calculations there is a 70% capacity factor built in whereas the present cases are for full power years, so his 10 years results should be looked at at the present 7-year values. Qualitatively all the features are close to that of Fig. 9a,b and c, except for ^{232}U that seems different in two respects. It has an almost flat region from 1 to 4 years, it rises after 4 years and appears to be increasing linearly with time and it is more than an order of magnitude lower than Fig. 9a (3×10^{-6}compared to 5×10^{-5}). Unfortunately, ^{231}Pa results were not given, however, Fig. 9a gives ^{228}Th of 2×10^{-6} at 30 y whereas, Fig. 12a

gives ~8×10^{-8}, again an order of magnitude lower. The value of $^{232}U/^{233}U$ at 30 y is about 0.4% whereas Fig. 9a shows about 5%. The present calculated values of $^{232}U/^{233}U$ is also about an order of magnitude higher for our all MS case and for the Be/MS case discussed next. Also, similar calculation give these higher values of $^{232}U/^{233}U$ >5% (Moir, Powers et al., 2009).

When full processing is assumed, removing both uranium and protactinium we compare our results, Fig. 9b with Berwald's in Fig. 12b. ^{232}U in Fig. 12b is 1.7×10^{-6} and Fig. 9b gives 2×10^{-6}. ^{228}Th in Fig. 12b at 30 y is 4×10^{-8} and Fig. 9b is 5×10^{-8}. Agreement is pretty good both qualitatively and quantitatively.

Be neutron multiplier/molten salt breeder /Be/MS

This example is another well documented design in Moir et al., 1984; Moir et al., 1985a; Moir et al., 1985b. A similar blanket design was done for a tokamak example (Moir et al., 1984c). These old studies did not calculate ^{232}U production. The cylindrical shell blanket is 127 m long and fusion power is 3000 MW. The neutron wall load is 2 MW/m^2 and blanket multiplication is 1.6. Fission especially of U-233 seems to increase the blanket energy multiplication. The first wall is at radius 1.5 m, 0.01 m of iron, the blanket extends from r=1.51 m to 2.1 and consists of 10 mm diameter beryllium spheres with molten salt circulating in steel tubes of 17 mm diameter. The molten salt is 70%LiF + 12% BeF_2+ 18% ThF_4, a 10 mm Fe wall extends to 2.11 m, graphite extends to 2.41 m. The blanket zone consists of 50vol% beryllium, 10% tubes, 0.8% Fe. The volume of molten salt inside the blanket is 85 m^3. We assume the volume outside is the same for a total volume of 170 m^3. The amount of thorium is 358 tonnes.

Table 7. Be/molten salt blanket parameters.

$P_{nuclear}$	4440 MW
P_{fusion}	3000 MW
$P_{alpha\ particle}$	600 MW
$P_{blanket}$	3840 MW
$P_{electric}$	1380 MW
$P_{wall\ load}$	2 MW/m^2
Length of blanket	127 m
First wall radius	1.5 m
T	1.1
F^*_{net}	0.6
M^*	1.6
Fissile production	6380 kg ^{233}U/yr at 80% capacity factor
Total cost	$4870 M (1982$)

*F_{net} is the fissile atoms bred/triton consumed
M is the energy released in the blanket per triton consumed divided by 14 MeV.

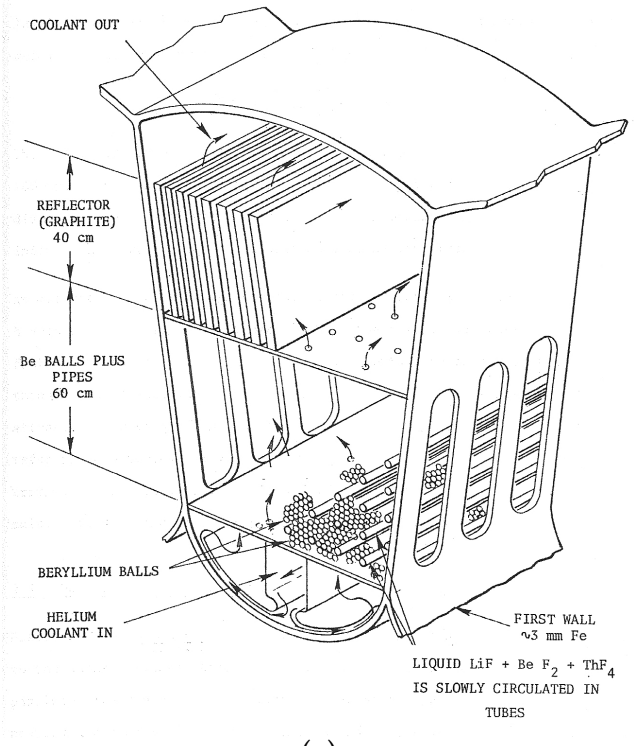

(a)

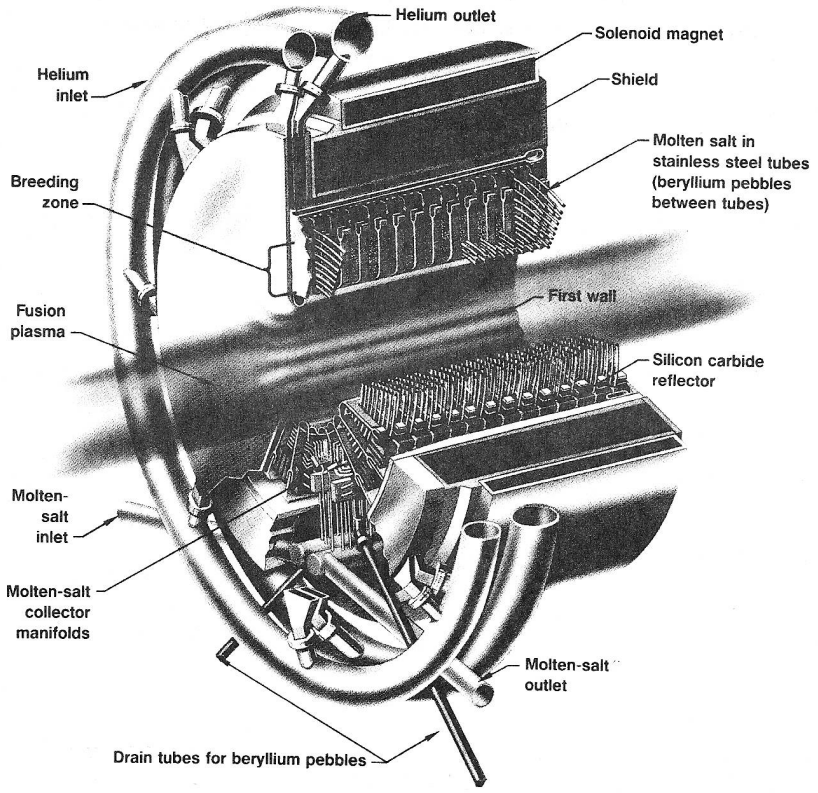

(b)

Fig. 13. Fission-suppressed blanket based on beryllium pebbles, showing the sub-module (a) and the module (b).

The TART calculations were done for spherical shell geometry and for an infinite cylinder. For both geometries unlike the documented designs above with a first wall at 1.5 m, the first wall was at 2.49 m with Fe to 2.5 m, with the beryllium spheres and a zone of molten salt carried in steel tubes out to 3 m, Fe wall out to 3.01 m and Graphite out to 3.5 m. The calculations, however, were done with no Fe in the walls, only in the molten salt zone. The different first wall radius should have only a small effect on the results.

The atom fractions in the molten salt zone at the start of the calculation are given in Table 8 along with those after the burn becomes close to steady state.

Table 8
Material percentages for the Be/MS blanket

Element	Atom, % t=0	Atom, % t=∞	Atom, % t=∞ with U238	Fission energy, MeV
6Li	0.02	0.02	0.02	
7Li	2.9325	2.9325	2.9325	
9Be	88.42	88.42	88.42	
19F	6.939	6.939	6.939	
56Fe	0.964	0.964	0.964	
228Th	0	1.08×10^{-6}	1.08×10^{-6}	
230Th	0.000752	0.00406	0.00406	0.015
232Th	0.752	0.752	0.752	1.56
231Pa	0.000752	0.00102	0.00102	0.014
232Pa	0.0000752	4.42×10^{-6}	4.35×10^{-6}	0.0007
233Pa	0.000752	0.00216	0.00217	0.009
232U	0.0000752	3.96×10^{-5}	3.96×10^{-5}	0.08
233U	0.000752	0.000895	0.000895	6.9
234U	0.000752	4.26×10^{-5}	4.26×10^{-5}	0.001
235U	0.0000752	7.13×10^{-7}	7.13×10^{-7}	0.005
238U	0.00498	0	0.00498	0.028
239Pu	0	0	1.98×10^{-4}	2.6
240Pu	0	0	6.34×10^{-5}	0.002

This equivalent calculation with $V_{outside}$=85 m^3, V_{inside} =85 m^3, with the processing rate being 10 m^3/d (17 days to process the entire molten salt inventory) shown in Fig. 14 and Table 3 and was varied to show the effect of energy release by fissioning of ^{233}U shown in Fig. 15.

The results are shown in Table 3 and Fig. 14. Adding the small amount of ^{238}U shown in Table 8 changed the reaction rates so little (for only 10^6 neutron

histories) that the same numbers from Table 3 were used with the additional results for ^{239}Pu and ^{240}Pu shown in Fig. 14.

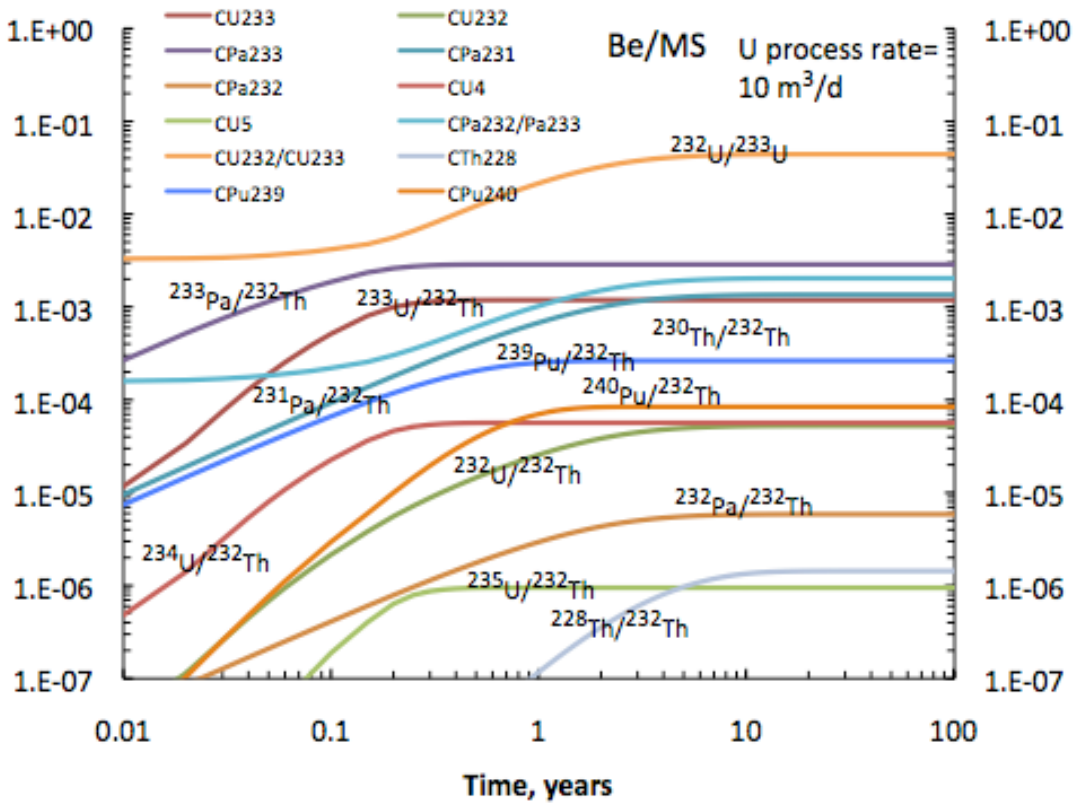

Fig. 14. Concentration ratios versus exposure time for the Be/MS case.

Denaturing with ^{238}U

By adding the right amount of ^{238}U to the molten salt the ^{233}U can be diluted to the low enriched uranium standard that is judged to be non-useful for bomb. This is <20% for ^{235}U and <12% for ^{233}U. Table 8 above gives the result of 11.8% ^{233}U in uranium that is extracted with the other numbers given. As uranium is extracted ^{238}U would have to be continuously added. The ratio of ^{238}U to Th is 0.00662 and needs to be continuously maintained by adding ^{238}U as it is extracted along with the other U isotopes. The amount of ^{232}Th should have been reduced in Table 8 by the amount of ^{238}U added which would have only a small effect on the results.

Table 9. (**redo with new numbers-only small changes expected)**
Contribution to the $^{232}U/^{233}U$ ratio in %, Be/MS

Time, y	Route #1 $^{233}Pa(n,2n)$	Route #2 $^{233}U(n,2n)$	Route #3 $^{232}Th(n,2n)$	Route #4 $^{232}Th(n,3n)$
0.05	3.0	0.07	96.8	0.09
0.1	2.6	0.13	97.0	0.2
0.2	2.0	0.16	97.4	0.45
0.5	0.9	0.09	97.5	1.5
1	0.5	0.05	96.2	3.2
5	0.27	0.026	86.8	12.9
10	0.25	0.025	83.6	16.1
20	0.25	0.025	83.0	16.7

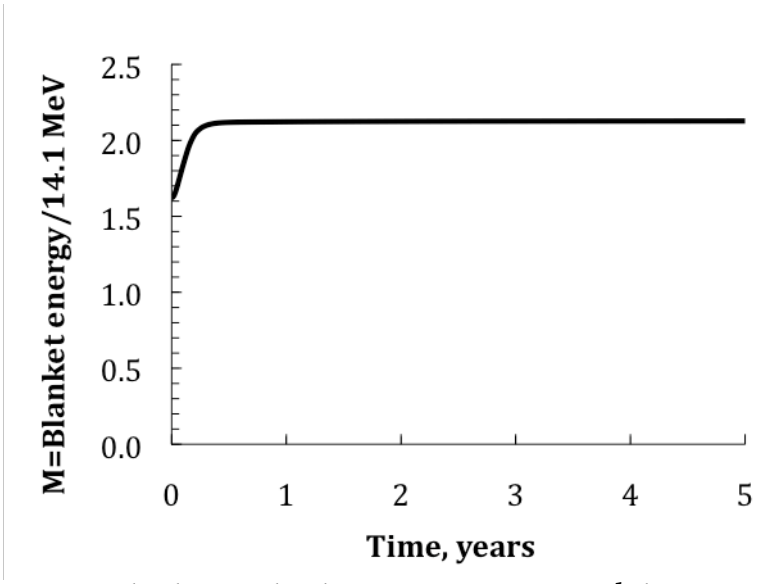

Fig. 15. Blanket multiplication increases with burn time.

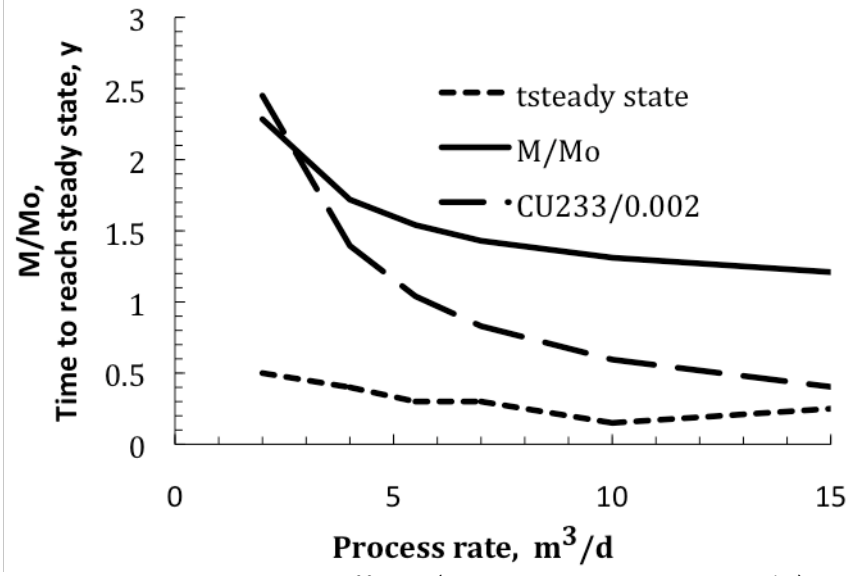

Fig. 16. Process rate effects (uranium processing only).

To keep the energy multiplication low, the process rate should be >5 m^3/d. Our example is 10 m^3/d with M=2.1. The old results in Table 7 are M=1.6 presumably they did not account for the buildup of fissile isotopes. From Table 8 we see the processing could be higher than 10 m^3/d in order to further reduce the fissioning of ^{233}U.

General comments

Although the calculations are done in 1-D spherical shell geometry and infinitely long cylindrical geometry, the results are thought to be applicable to other geometry such as a tokamak as long as the power/molten salt volume ratio is similar. The breeding rate, [Th(n,2n) reactions] will not be too accurate because of the simplifying assumptions such as no first wall and no holes, especially for the all MS case. But the production of U-232 should be fairly characteristic of more accurate calculations. The Li/MS case will have significant differences as the examples show. More accurate calculations would include holes, wall material and more structural materials. The first wall of a few mm thickness up to 10 mm should be included but will only have a marginal impact on the results. A line source appropriate to a cylinder will have neutrons impacting the first wall and beyond more obliquely rather than all perpendicular as in spherical geometry that explains some differences of a line source and a point source. Again this should change numbers on the margin. High values of U-233 and other isotopes (see Table 8) results in energy release from fission causing the power to rise and at a fixed total power, the fusion power will have to be lowered thereby lowering the U-233 production rate.

If we desire to lower the U-233 fission rate we can process U at a higher rate to lower the U-233 density. If we desire to limit the Pa-231 concentration we could process the Pa to keep the Pa at a fixed value. This processing rate would be quite low; however, it would have proliferation implications. By adding ^{238}U, ^{232}U /(^{233}U+ ^{238}U) can be kept <12% if desired.

Discussions and conclusions

The disagreement of these results with those of Berwald's means we must be on alert for a systematic error in all the results. Resolving this discrepancy is an important topic for further study. However, there is enough evidence based on independent calculations for ^{232}U /^{233}U values of 5% and more after several years of exposure so that we can cautiously proceed. There are two options: 1- produce ^{233}U with ~5% ^{232}U for use in pure thorium cycle fission reactors or 2- produce ^{233}U along with 5% ^{232}U both diluted with ^{238}U so $^{233}U/U$ is 12% that is not useful for bombs. The results in this report should be useful in conducting proliferation risk/nuclear power benefit studies of a fusion fuel breeder based on either magnetic or inertial fusion reactors feeding fission reactors.

Acknowledgements

The help from D. E. Cullen in getting the TART code up and running is greatly appreciated.

References

D. H. Berwald, Chapter VII, especially Table VII.C-4 and pages VII-69 to 87, Fuel Cycle Technologies of J. D. Lee, et al., "Feasibility Study of a Fission-Suppressed Tandem-Mirror Hybrid Reactor", Lawrence Livermore National Laboratory, Livermore, CA, UCID-19327 (1982).
http://ralphmoir.com/media/uCID19327pt1sm.pdf
http://ralphmoir.com/media/uCID19327pt2sm.pdf

D.E. Cullen, "TART 2005: A Coupled Neutron-Photon 3-D, Time Dependent, Combinatorial Geometry Monte Carlo Transport Code," Lawrence Livermore National Laboratory, UCRLSM-218009, November 22, 2005. The calculations were done with the latest version of TART and with the ENDFB-7 nuclear data files.

J. Kang and F. N. von Hippel, "U-232 and the proliferation resistance of U-233 in spent fuel," *Science & Global Security*, **9** (2001) 1-32.

C. Le Brun, L. Mathier, D. Heuer and A. Nuttin, "Impact of the MSB concept technology on long-lived radio-toxicity and proliferation resistance," Note LPSC 05-81 (2005). Proceeding of " *Technical Meeting on Fissile Material Management Strategies for Sustainable Nuclear Energy*, Vienna: Austria (2005)."

B. R. Leonard, Jr and U. P. Jenquin, "The quality of fissile fuel bred in a fusion reactor blanket," Proceedings of The Second Topical Meeting on the Technology of Controlled Nuclear Fusion, Sept 21-23, 1976, Richland, Washington, Vol. II p 711-722. Reference not used.

R. W. MOIR and T. D. ROGNLIEN, "Axisymmetric tandem mirror magnetic fusion energy power plant with thick liquid-walls" *Fusion Science and Technology* **52**, (2007) 408-416.

R. W. Moir, et al., "Helium-Cooled Molten Salt Fusion Breeder", Lawrence Livermore National Laboratory, Livermore, CA, UCID-20153 (1984a).

R. W. Moir, et al., "Helium-Cooled Molten Salt Fusion Breeder", Tandem Mirror, Lawrence Livermore National Laboratory, Livermore, CA, UCID-20153 (1984b), 204 pages.

R. W. Moir, et al., "Feasibility Study of a Fission-Suppressed Tokamak Fusion Breeder", Tokamak, Lawrence Livermore National Laboratory, Livermore, CA, UCID-20154 (1984c).

R. W. Moir, et al., "Helium-Cooled Molten Salt Fusion Breeder" *Fusion Technology*, **8**, (1985a), 8 pages.

R. W. Moir, et al., "Design of a Helium-Cooled Molten Salt Fusion Breeder", Fusion Technology, Vol. 8, No. 1 Part 2(A) 465 (1985b).

R. W. Moir, U232 nonproliferation features, (June 25, 2010) *Vallecitos Molten Salt Research*, Report No. 2, 17 pages

R. W. MOIR, H. F. SHAW, A. CARO, LARRY KAUFMAN, J. F. LATKOWSKI, J. POWERS, P.E. A. TURCHI, "MOLTEN SALT FUEL VERSION OF LASER INERTIAL FUSION FISSION ENERGY (LIFE)," FUSION SCIENCE AND TECHNOLOGY VOL. **56** (2009).

Edward I. Moses, Tomas Diaz de la Rubia, Erik Storm, Jeffery F. Latkowski, Joseph C. Farmer, Ryan P. Abbott, Kevin J. Kramer, Per F. Peterson, Henry F. Shaw and Ronald F. Lehman II, "A SUSTAINABLE NUCLEAR FUEL CYCLE BASED ON LASER INERTIAL FUSION ENERGY," *FUSION SCIENCE AND TECHNOLOGY* **56** (2009).

P.Oblozinsky and M.Herman, Editors, "ENDF/B-VII.0: Next Generation Evaluated Nuclear Data Library for Nuclear Science and Technology", Nuclear Data Sheets 107 pp. 2931-3060

Somayajulu and Church, "Radium, Thorium, and Uranium Isotopes in the Interstitial Water from the Pacific Ocean Sediment," *Journal of Geophysical Research* **78** (1971) 4529-4531.

Appendix A— Approximations for early and late times

For early times, the approximate ratios are:

$$\frac{dC_{P3}}{dt} \approx R_{Th}K \qquad C_{P3} \approx R_{Th}K\,t \quad for\ t << 27\,d$$

$$C_{P3} \approx R_{Th}K\,t \quad for\ t >> 27\,d$$

for the Li/MS case

$$C_{P3} = \frac{R_{Th}K}{R'_{P3}K + \lambda_{P3} + F^{Pa}\eta_{Pa}} = \frac{0.515 \times 2.76 \times 10^{-10}}{9.63 \times 2.76 \times 10^{-10} + 2.97 \times 10^{-7}} = 0.000474$$

$for\ t >> 27\,d$

At a 70% capacity factor this would be 0.00033 in good agreement with Fig. 12a.

$$\frac{dC_{P1}}{dt} \approx R'_{Th}KC_{Th} \qquad C_{P1} \approx R'_{Th}K\,t$$

$$\frac{dC_{Th230}}{dt} \approx R''_{Th} K \qquad C_{Th230} \approx R''_{Th} K\, t$$

$$\frac{dC_{U3}}{dt} \approx \lambda_{P3} R_{Th} K\, t \qquad C_{U3} \approx \lambda_{P3} R_{Th} K\, t^2/2$$

$$C_{U3} \approx 2.97\times10^{-7} \times 0.254 \times 3.4\times10^{-10}\, t^2/2$$
$$\approx 1.28\times10^{-17}\, t^2 \ in\ s$$
$$\approx 0.01275\, t^2 \ in\ y$$

In good agreement with Fig. 9a. Fig. 12a is based on a 70% capacity factor and seems to initially rise faster than t^2.

$$\frac{dC_{U2}}{dt} \approx R_{P1} K C_{P1} + R_{P3} K C_{P3} + \ldots \qquad C_{U2} \approx (R'_{Th} R_{P1} + R_{Th} R_{P3}) K^2 t^2/2$$

$$\frac{C_{U2}}{C_{U3}} \approx \frac{(R'_{Th} R_{P1} + R_{Th} R_{P3}) K}{R_{Th} \lambda_{P3}}$$

$$C_{U2} \approx (R'_{Th} R_{P1} + R_{Th} R_{P3}) K^2 t^2/2$$
$$\approx (0.0246\times12.85 + 0.515\times0.025) \times (2.76\times10^{-10})^2 t^2/2$$
$$\approx (1.2\times10^{-20} + 0.098\times10^{-20})\, t^2 \quad for\ t\ in\ s\ for\ t < 27\, d$$
$$\approx 1.3\times10^{-5}\, t^2 \quad for\ t\ in\ y\ for\ Li/MS\ case$$

$$for\ t > 27\, d$$

$$C_{U2} \approx R'_{Th} R_{P1} K^2 t^2/2 + \frac{R_{Th} R_{P3}}{\lambda_{P3}} K^2 t + \text{constant}$$
$$\approx 1.2\times10^{-20}\, t^2 + \frac{0.515\times0.025}{2.97\times10^{-7}} (2.76\times10^{-10})^2\, t + 0.98\times10^{-17}$$
$$\approx 1.2\times10^{-20}\, t^2 + 0.033\times10^{-14}\, t + 1.0\times10^{-8} \quad for\ t\ in\ s$$
$$\approx 1.2\times10^{-5}\, t^2 + 1.04\times10^{-8}\, t + 1.0\times10^{-8} \quad for\ t\ in\ y$$

In good agreement with Fig. 9a,b and c. Fig. 12a is based on a 70% capacity factor and has the right slope but seems off vertically by some amount.

$$\frac{C_{U2}}{C_{U3}} \approx \frac{(0.196\times1.05 + 0.254\times0.21)\times3.4\times10^{-10}}{0.254\times2.97\times10^{-7}} = 0.00117$$ MS example, Fig. 5 gives

0.00113 for good agreement.

$$\frac{C_{U2}}{C_{U3}} \approx \frac{(0.0246\times12.85 + 0.515\times0.025)\times2.76\times10^{-10}}{0.515\times2.97\times10^{-7}} = .000594$$ Li/MS example,

Fig. 9a, b, c gives 0.0006 for good agreement.

$$\frac{C_{U2}}{C_{U3}} \approx \frac{(0.0267 \times 23.56 + 0.78 \times 0.028) \times 11.4 \times 10^{-10}}{0.78 \times 2.97 \times 10^{-7}} = 0.0032$$ Be/MS example, Fig. 14 gives 0.00326 for good agreement.

For late times when steady state occurs the ratios are:

$$C_{Th230} = \frac{R''_{Th}}{R'_{Th230}} = \frac{0.052}{0.43} = 0.121 \; or \; \frac{0.00229}{8.07} = 0.000284; \frac{0.0054}{10.0} = 0.00054$$ good agreement for the 3 cases

$$C_{P3} = \frac{R_{Th}K}{R'_{P3}K + \lambda_{P3} + F^{Pa}\eta_{Pa}} = \frac{0.254 \times 3.4 \times 10^{-10}}{0.21 \times 3.4 \times 10^{-10} + 2.97 \times 10^{-7}} = 0.0002907$$ MS example good

$$C_{P3} = \frac{R_{Th}K}{R'_{P3}K + \lambda_{P3} + F^{Pa}\eta_{Pa}} = \frac{0.515 \times 2.76 \times 10^{-10}}{9.63 \times 2.76 \times 10^{-10} + 2.97 \times 10^{-7}} = 0.000474$$ for Li/MS case

$$C_{U2} = \frac{^{232}U \; atoms}{^{232}Th \; atoms}; \quad \frac{dC_{U2}}{dt} \approx 0$$

$$C_{U2} \approx \frac{R_{P1}KC_{P1}}{R'_{U2}K + F^{U}\eta_{U}}; \quad R'_{U2}K << F^{U}\eta_{U}; \quad C_{P1} \approx \frac{R'_{Th}}{R'_{P1}}$$

$$C_{U2} \approx \frac{R_{P1}R'_{Th}K}{F^{U}\eta_{U}R'_{P1}}$$

$$C_{U2} \approx \frac{R_{P1}R'_{Th}K}{F\eta_{U}R'_{P1}} \approx \frac{12.85 \times 0.0246 \times 2.76 \times 10^{-10}}{1.447 \times 10^{-7} \times 12.91} \approx 4.67 \times 10^{-5}$$ In good agreement with Li/MS case of Fig. 9a. but not good agreement with Fig. 12a as can be seen from the red dashed horizontal line of Fig. 12a.

$$C_{U3} \approx \frac{\lambda_{P3}C_{P3}}{R'_{U3}K + F^{U}\eta_{U}}; \quad C_{P3} \approx \frac{R_{Th}K}{R'_{P3}K + \lambda_{P3}}$$

$$C_{U3} \approx \frac{\lambda_{P3}}{R'_{U3}K + F^{U}\eta_{U}} \frac{R_{Th}K}{R'_{P3}K + \lambda_{P3}}; \quad R'_{U3}K << F^{U}\eta_{U}; \quad R'_{P3}K << \lambda_{P3}$$

$$C_{U3} \approx \frac{R_{Th}K}{F^{U}\eta_{U}}$$

$$C_{U3} \approx \frac{0.254 \times 3.4 \times 10^{-10}}{2.38 \times 3.4 \times 10^{-10} + 3.036 \times 10^{-7}} = 0.284 \times 10^{-3}$$

Good agreement with MS case of Fig. 5.

$$C_{U3} \approx \frac{0.515 \times 2.76 \times 10^{-10}}{14.55 \times 2.76 \times 10^{-10} + 1.447 \times 10^{-7}} = 0.982 \times 10^{-3}$$

Good agreement with Li/MS case of 9a and 12a.

$$C_{U3} \approx \frac{0.78 \times 11.4 \times 10^{-10}}{32.65 \times 11.4 \times 10^{-10} + 6.808 \times 10^{-7}} = 1.306 \times 10^{-3}$$

Good agreement with Be/MS case of Fig. 14.